INVESTIGATION OF THE EFFECT OF THE SPACING BETWEEN ORIFICES ON THE DAMPING PERFORMANCE IN PASSIVE-TUNED LIQUID COLUMN DAMPERS

A Thesis Submitted to
the Graduate School of
İzmir Institute of Technology
in Partial Fulfilment of the Requirements for the Degree of

MASTER OF SCIENCE

in Mechanical Engineering

by

Ozan KARAKUŞ

July 2024
İZMİR

We approve the thesis of **OZAN KARAKUŞ**

Examining Committee Members:

Assoc. Prof. Dr. Ünver ÖZKOL
Department of Mechanical Engineering, IZTECH

Assist. Prof. Dr. Doğan KISACIK
Department of Civil Engineering, IZTECH

Assoc. Prof. Dr. Utku ŞENTÜRK
Department of Mechanical Engineering, Ege University

12 July 2024

Assoc. Prof. Dr. Ünver ÖZKOL
Supervisor, Department of Mechanical Engineering, IZTECH

Prof. Dr. M. İ. Can DEDE
Head of the Department of Mechanical Engineering, IZTECH

Prof. Dr. Mehtap EANES
Dean of the Graduate School

ABSTRACT

INVESTIGATION OF THE EFFECT OF THE SPACING BETWEEN ORIFICES ON THE DAMPING PERFORMANCE IN PASSIVE-TUNED LIQUID COLUMN DAMPERS

Damping systems are designed to stabilize the structures by concerning any types of external excitations that can occur. Decreasing the structural movements is extremely important for structures to preserve their integrity. Passive Tuned Liquid Column Dampers -TLCD- are preferred systems in practice due to their simple structures and not requiring an external energy input and therefore, they can be effectively used in the suppression of structural oscillations.

In this thesis, the damping performance of a TLCD was studied, specifically considering the effect of the head loss coefficient on the performance of a liquid column. An analytical model was produced, and the equation of motions was solved in 1D. Experiments were performed to confirm the analytical solutions and to gain information where the analytical model was not sufficient in the case of two orifices that were close to each other. An experimental design was used to obtain the head loss value of the tuned liquid column damper. A series of experiments were completed to observe the effect of the head loss coefficient on the damping performance of the tuned liquid column dampers. According to experimental and analytical results, a relation between the damping ratio of the system and the head loss coefficient of the damper was noted.

It was experimentally monitored that there is an optimum spacing between two orifices where the performance of the TLCD may be maximized. It was also noted that, according to experiments damping ratio of the system was improved by 10.5%.

ÖZET

PASİF AYARLI SIVI KOLON SÖNÜMLEYİCİLERDE DELİKLER ARASINDAKİ BOŞLUĞUN SÖNÜMLEME PERFORMANSINA ETKİSİNİN İNCELENMESİ

Yapısal hareketler, sönümleyici tasarımı ve bunların ilişkileri yapı dinamiğinin ana konularıdır. Sönümleme sistemleri, oluşabilecek her türlü dış uyartımı dikkate alarak yapıları stabilize etmek için tasarlanmıştır. Yapısal hareketlerin azaltılması yapıların bütünlüğünü koruyabilmesi açısından son derece önemlidir. Bu sönümleme sistemleri genel olarak aktif ve pasif sönümleme sistemleri olmak üzere iki sınıfta toplanır. Pasif Ayarlı Sıvı Kolon Sönümleyiciler -TLCD- basit yapıları ve dışarıdan bir enerji girişi gerektirmemesi nedeniyle pratikte tercih edilen sistemlerdir ve bu nedenle yapısal salınımların bastırılmasında etkin bir şekilde kullanılabilirler.

Bu tezde, TLCD'nin sönüm performansı, özellikle yük kaybı katsayısının sıvı kolon performansı üzerindeki etkisi dikkate alınarak incelenmiştir. Analitik bir model üretildi ve hareket denklemi 1 boyutlu olarak çözüldü. İki deliğin birbirine yakın olması durumunda analitik çözümlerin doğrulanması ve analitik modelin yeterli olmadığı durumlarda da bilgi elde etmek amacıyla deneyler yapılmıştır. Yük kaybı katsayısının hesaplanması birçok çalışmada araştırılmış ve ampirik formülasyonlar önerilmiştir, ancak sıvı kolonun yük kaybı değeri bir dizi deney uygulanarak elde edilebilir. Ayarlanmış sıvı kolon damperinin yük kaybı değerini elde etmek için deneysel bir tasarım kullanıldı. Yük kaybı katsayısının, ayarlanmış sıvı kolon damperlerinin sönümleme performansı üzerindeki etkisini gözlemlemek için bir dizi deney tamamlandı. Deneysel ve analitik sonuçlara göre sistemin sönüm oranı ile damperin yük kayıp katsayısı arasında bir ilişki tespit edilmiştir.

TLCD'nin performansının maksimuma çıkarılabileceği iki delik arasında optimum bir aralık olduğu deneysel olarak tespit edilmiştir. Ayrıca deneysel sonuçlara göre sistemin sönümleme katsayısının %10.5 oranında geliştiği not edilmiştir.

TABLE OF CONTENTS

LIST OF FIGURES vii

LIST OF TABLES ix

LIST OF SYMBOLS x

CHAPTER 1. INTRODUCTION 1
1.1 History of Object Motion 2
1.2 Characteristics Features of Structure Behaviours 2
1.3 Types of External Excitations for Structures 2
1.4 Motion and Vibration Mitigation Methods and Absorber Types 4
1.4.1 Passive Tuned Mass Dampers and Passive Tuned Liquid Column Dampers 5
1.4.2 Tuned Mass Dampers Applications 7
1.4.3 TLCDs Applications in Floating Offshore Wind Turbines 7
1.4.4 Orifice Effect on Damping Performance of TLCD 11
1.5 Motivation 12

CHAPTER 2. ANALYTICAL AND NUMERICAL METHODOLOGY 14
2.1 Determining Equation of Motion for Linear Damped Single Degree of Freedom System 14
2.2 Determining of Equation of Motion for TLCD 16
2.3 Analytical Model Coupled Primary Structure and TLCD 18
2.4 Head Loss Coefficient and Orifice of TLCDs 21

CHAPTER 3. EXPERIMENTAL METHODOLOGY 23
3.1 Experimental Design 23
3.2 Explanation of Experimental Process and Data Collection 26
3.3 Determining Physical Properties of Structure and TLCD with Experiment 27

CHAPTER 4. RESULTS 30
4.1 Damping Performance of TLCD in Relation to Head Loss Coefficient 30
4.2 Experimental Investigation of the Effect of the Distance Between Orifices 34

CHAPTER 5. CONCLUSION 37

REFERENCES 38

APPENDICES
APPENDIX A. Visual of Experimental Desing 40
APPENDIX B. Video Analysis Process 41
APPENDIX C. Python Code for Solution of Analytical Modeling 42

LIST OF FIGURES

Figure **Page**

Figure 1.1 Diagram of the limited DOF model for the monopile 5

Figure 1.2 Displacement time story of a Tension Leg Floating Platform with and without TLCD damper 8

Figure 1.3 50 scale Tension Leg Platform and three different TLCDs 9

Figure 1.4 Comparison of time response between simulation and experimental results 10

Figure 2.1 A single degree of freedom system (a) and free body diagram (b) 14

Figure 2.2 A U-Shape TLCD 17

Figure 2.3. Analytical model of a coupled structure and absorber system TLCD is located 18

Figure 2.4 Algorithm for the solution of analytical model 20

Figure 2.5 Head loss coefficient calculation with respect to opening ratio of cross-section 22

Figure 3.1 Technical Drawing of the Structure 24

Figure 3.2 Technical Drawing of the U-Shape TLCD 25

Figure 3.3 Structure displacement-time story without damper 28

Figure 3.4 Visual of experimental setup 29

Figure 4.1 Decay plots of coupled system from analytical results with respect to different head loss coefficients 31

Figure 4.2 TLCD and extra orifices 32

Figure 4.3 Decay plots of coupled system from experiment for one and three orifices 33

Figure 4.4 Damping ratios of coupled system with respect to different head loss values 33

Figure 4.5 Damping ratio with respect to orifice diameter over orifice spacing.....35

Figure 4.6 Decay plots of coupled system concerning distance between orifices 36

Figure A.1 Visual of experimental design..... 40

Figure B.1 Visual from tracker screen.....41

LIST OF TABLES

Table **Page**

Table 3.1 Structure mechanical specifications and their values. 27

Table 3.2 Mechanical properties of TLCD 28

Table 4.1 Damping ratios of coupled system with respect to different head loss coefficients. 31

Table 4.2 Damping ratio values with respect to distance between orifices 35

LIST OF SYMBOLS

Nomenclature

Symbol	**Meaning**	**Unit**
F	Force	N
m	Mass	kg
v	Velocity	m/s
x	Displacement	m
t	Time	s
$\ddot{x}$	Acceleration	m/s^2
$\dot{x}$	Velocity	m/s
A	Cross-sectional area	m^2
L	Length of liquid column	m
B	Length of horizontal liquid column	m
g	Gravitational acceleration	m/s^2
M	Mass	kg
u	Displacement value of numerical steps	m
$\dot{u}$	Velocity value of numerical steps	m/s
$\ddot{u}$	Acceleration value of numerical steps	m/s^2
h	Numerical increment value	-
TLCD	Tuned Liquid Column Damper	-
TMD	Tuned Mass Damper	-
DOF	Degree of freedom	-

Greek Letters

Symbol	**Meaning**	**Unit**
ω	Angular velocity	rad/s
ζ	Damping ratio	-
ρ	Density	kg/m^3
η	Head loss coefficient	-

β	Area ratio of cross-sectional to orifice	-

Subscripts and Superscripts

Symbol	**Meaning**	**Unit**
k	Stiffness force	N
c	Damping force	N
cr	Critical damping	Ns/m
s	Structure	-
f	Fluid	-
fh	Horizontal part of fluid	-
n	Number of steps	-

CHAPTER 1

INTRODUCTION

The liquid damper is a type of absorption mechanism that is effectively used to control the structural motions which can occur as oscillation or vibration. These structural motions can be kept in a safe region by using any appropriate damping mechanism by considering structure and damper properties and their relations. The relation between structural motion, dampers, external excitation, and mechanical properties of a structure is the subject of structural dynamics where the response of a structure is calculated as displacement, velocity, and acceleration by solving a series of differential equations called equations of motion. Equations of motion describe the behaviour of the physical system in terms of its response concerning time by considering the mechanical properties of a structure with external forces concerning a defined reference location. Vibrational structural motions are affected by elasticity, mass, and geometrical properties which result in a vibrational frequency specific to the structure called natural frequency. When a structure is forced at this natural frequency, vibrational amplitudes grow rapidly, which is called structure resonating, and this situation usually fails the structural integrity. Due to these resonance phenomena, structures must be designed by decoupling forcing and natural frequencies away from each other. All these motions of the structures that occur due to the external excitations should be monitored and controlled to keep structures response in a safe region if they cannot be avoided.

In practice, some solutions are already used to reduce the response of the structures by utilizing motion mitigation strategies such as tuned mass dampers, pendulums, tuned liquid dampers, tuned liquid column dampers, gyroscopes, and viscoelastic dampers. Tuned liquid column dampers are operative absorption mechanisms that are properly used to monitor structural responses in controlling wind, wave, or seismic-induced motions. These types of absorbers can be effectively applied to a structure by sizing its features concerning the mechanical properties of the structure and external excitation conditions. The motion of structure can be a topic of discussion in structural dynamics such as a simple beam or a complicated twenty-storey building, or a

floating vessel, or a complicated structure of a floating wind turbine, its mooring, platform, and tower. One of the many challenges here is to define the dynamic parameters of these absorbers. When designing an absorber, one of the motion indicators, such as the displacement of the top of a structure or the acceleration of some specific points should be selected as the target of the design and the absorber should be designed to minimize that target.

1.1 History of Object Motion

Objects and their behaviours have always been interesting topics in human history. Greek philosopher Aristotle (384–322 BC) hypothesized that heavier objects would fall more quickly to the surface of the earth than lighter ones. However, Galileo (1634) testified that two different objects fall at the same time even if one object is heavier than the other one. Newton (1687) invented and formulated gravitational theory. Einstein explained all these relationships with the theory of general Relativity in a more complete manner. However, all these theories and observations can help us to explain the behaviour of objects. Classical mechanics and equations of motion can be used to calculate a structure`s behaviours if objects move much slower than the speed of light.

1.2 Characteristics Features of Structure Behaviours

Due to different mass and stiffness values, the natural frequency of each part of a structure causes different deflection patterns which shows relative displacement between these parts. When response of the structure is calculated under any excitation these deflection patterns should be considered for precise response. Direction and frequency of excitation are also important factors that change response of the structure.

1.3 Types of External Excitations for Structures

The excitations on structures can arise from various sources and can be classified into several types based on their origin and characteristics.

Seismic Waves: The frequency of these waves varies in a wide range and specifically occurs due to the earthquake having different amplitudes, and directions. The

frequency magnitude of seismic waves can be large as high as the audible range on the other hand seismic excitations can also be observed at low frequencies. The displacement amplitude of seismic excitations can also reach up to 0.1 meters.

Wind-induced excitations which occur due to the airflow around a structure can cause oscillations that are dependent on wind speed, direction, turbulence of flow, and aerodynamic characteristics of structures. Tall buildings, bridges, towers, and wind turbines are particularly susceptible to wind-induced vibrations. When a fluid flows around a solid surface, a boundary layer flow forms on its solid surfaces. When boundary layer separation occurs due to adverse pressure gradients, it causes regular shedding vortices, also known as a Karman vortex street, which is named after the engineer Theodore von Karman. These shedding vortices cause a dynamic pressure field around the body which eventually results in buffeting of the structure. This vortex shedding can be devastating for structures when the structure`s natural frequency and the shedding frequency of the vortex match, which is also called resonance. Vincenc Strouhal (1878), who experimented with oscillating flows, found out the vortex-shedding mechanisms of this buffeting behaviour. He realized that a nondimensional group, now called the Strouhal number, is the main parameter that describes the vortex-shedding mechanism along with the Reynolds number.

Traffic-induced excitations can, for example, be very important in the designs of pedestrian overpasses. They occur due to vehicle speed, weight, suspension characteristics of vehicles, and road surface conditions.

Machinery operations can also cause many cyclic loadings in buildings or bridges. Structures are subjected to dynamic loadings due to rotating machines, electric motors, pumps, or industrial processes. These excitations generally lead to structural vibrations, resonances, or fatigue failures if not properly controlled.

Waves, including hydrodynamic pressures and inertial forces, exert a dynamic impact on the structure of floating platforms. Excitations due to ocean waves, which cause periodic external loadings for floating and fixed structures, can be classified under different titles in terms of their period and the height of waves. These forces may lead to structural fatigue and possible damage over time, by causing the platform to bend, twist or turn in an oscillating way. The waves interact with the platform's body, jacking systems, and any supporting components leading to complicated interaction of wave structures. These interactions may result in resonant responses, dynamic amplifications, and nonlinear effects that need to be carefully considered when a platform is designed and

operated. Due to the changes in underwater topography speed, period, and height of the ocean waves start bending wavefronts. Wave reflection which occurs due to the reflective boundary can also contribute to the standing waves is another negative situation in stabilization of floating platforms. All these complexities and irregular behaviours of ocean waves cause complicated excitations which should be monitored and absorbed on floating platforms.

1.4 Motion and Vibration Mitigation Methods and Absorber Types

As mentioned in previous titles all structures have an oscillation due to their natural frequency and external forcing perturbations. In order to control these oscillations and vibrations some techniques and systems are used which aim at mitigating or controlling them within the structure. These methodologies are generally classified as active, semi-active, and passive control systems.

Active absorber systems are relatively complicated damping systems that require sensors, actuators, and control to actively monitor structural movements in real-time and reduce structural oscillations or vibrations. In this way, optimum and adaptable motion mitigation can be provided. The oscillation amplitude or frequency of a structure is monitored to apply the optimum amount of damping required. Unfortunately, despite all its benefits, an active absorption system requires an energy supply, consists of complex parts, and has a maintenance cost that is usually high.

Passive absorber systems reduce the structural motions by inherently dissipating their kinetic energy without using any external power source, sensors, or actuators. These systems are widely preferred due to their relatively simple structures, and low maintenance costs.

However, the design parameters of passive absorbers should be accurately defined with respect to the properties of the structure, excitation conditions, and exposed forces to obtain the best mitigation response. Passive-tuned mass dampers and passive-tuned liquid dampers are two widely used passive absorber methods due to their effectiveness and basic designs. Stewart and Lackner (Stewart et al. 2013) concluded that the tower fatigue reductions could reach up to 20% for the optimized tuned mass damper in offshore wind turbines either fixed or floating. A TMD was located inside the nacelle shown in Figure 1.1 and the parameters of the TMD were calculated for better damping performance.

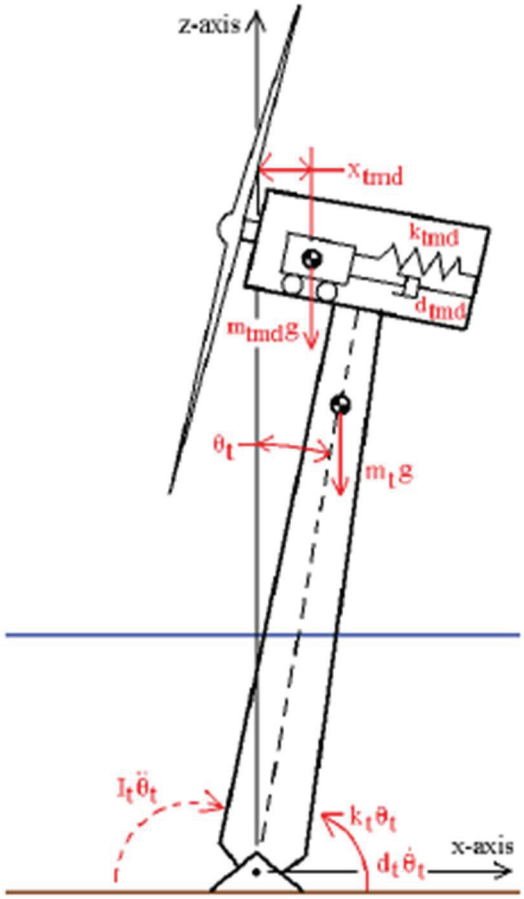

Figure 1.1 Diagram of the limited DOF model for the monopile.
(Source: Gordon Stewart et al. 2013)

Semi-active absorber systems are a combination of both active and passive systems. In these systems, damping properties can be adjusted using real-time sensor feedback as much as possible like active systems. However, semi-active absorbing systems do not require as much power as fully active systems. Semi-active systems balance complexity and performance; while complexity and power requirements are lower than active systems, the motion mitigation capabilities in structures can be efficient as active systems.

1.4.1 Passive Tuned Mass Dampers and Passive Tuned Liquid Column Dampers

Passive Tuned Mass Dampers -TMD- are used to mitigate the oscillations and vibrations by implementing a secondary mass to the structure through springs and

dampers. The amplitude of the structure`s motions is reduced by absorbing its kinetic energy onto secondary mass and dissipating through the friction in the damper. The secondary mass is generally a heavy steel part or a concrete block. The weight of the secondary mass should be carefully determined based mainly on the mass of the main structure, where it should not increase the total mass of the structure much and the desired reduction of the oscillation and motion.

The mass of the absorber and its natural frequency of TMD are calculated with respect to the primary structure`s frequency that is being suppressed. The natural frequency of a TDM should be matched with the forcing frequency to absorb most of its kinetic energy. A mass damper tuned this way has a 180-degree phase difference with the structure. The damping mechanism of TMDs is defined with respect to the amount of the dissipated energy by dampers. Thereby, the kinetic energy of the secondary mass is converted to temperature. The location and direction of TMD are also important parameters in applications, which depend on parameters such as structure dynamic properties and vibration modes.

Tuned liquid dampers are also effectively used to mitigate the motions of structures. When external excitations are applied to the structure, these motions are directly transferred to the tuned liquid dampers that are located inside the structure. They dissipate kinetic energy by utilizing the sloshing of liquid within a container. The sloshing mechanism causes a periodic liquid motion inside the container, which has an opposite motion relative to the structure if designed correctly. As the liquid sloshes, its energy is dissipated by viscous damping. Tuned liquid damper`s specifications should be defined such as container geometries or liquid density. Despite the benefits of tuned liquid dampers in suppressing structural oscillations and vibrations, space requirements for installation can be a problem.

TLCDs are a subclass of tuned liquid dampers which have a U-shape geometry. Two vertical columns are oriented with a horizontal channel. These dampers are especially used to mitigate wind or wave-induced oscillations where periodicity is dominant. The cross-sectional geometry of U-shapes is generally designed as a circle; however, it can be a rectangle or square, too. Diameters of horizontal and vertical columns, length of the horizontal part, and total liquid column are some of the design parameters of tuned liquid column dampers which should be detailed and determined. Stiffness and damping values of column dampers are also dependent on these parameters. These dampers do not need separate parts like stiffness or dampers. These values are

inherently produced by liquid columns. TLCDs also do not occupy too much place as tuned liquid dampers do.

Energy is dissipated by wall friction and some sloshing on the free surfaces. To optimize the amount of damping, the head loss coefficient of liquid motion must be determined by calculating shear stresses in the moving liquid. The amount of head loss can be increased by implementing extra fins, flaps, or orifices inside the channels. The oscillation frequency of tuned liquid column dampers is proportional to the total length of the liquid column.

1.4.2 Tuned Mass Dampers Applications

Sadek and co-workers (Sadek et al. 1997) obtained that a TMD in reducing of displacement and acceleration responses of structure can reach up to 50 percent with proposed damper parameters while the structure is subjected to seismic excitations. Zou and co-workers (Zuo et al. 2017) concluded that peak response mitigation of structure can also reach up to 48.01 percent by using six tuned mass dampers while the floating platform and the turbine are subject to wind and wave excitations.

The direction of excitations and structure responses should be also considered in absorption applications. To reduce the pitch and roll motion of a floating offshore wind turbine under wind-induced excitation, two perpendicular TMDs which are located at the nacelle are studied by Lackner and co-workers (Lackner et al. 2011), and pitch and roll motion reduction values were obtained up to 12.5 percentage degree and 14.2 percentage degree respectively. As shown in previous research TMDs can be effectively used to mitigate the response motions of structures under different types of excitations, regardless of their location either on land or in the sea.

1.4.3 TLCDs Applications in Floating Offshore Wind Turbines

Floating offshore wind turbines are subjected to wind and waves at the same time. The high flexibility of floating offshore wind turbines makes them extra fragile; these vibrations and oscillations should be mitigated to ensure not only the turbine`s safe operation but especially its operation with low maintenance throughout its lifespan. For this purpose, structure`s movements should be mitigated by platform design, dampers, or

both. In literature, numerical studies have shown that the motion of a floating offshore wind turbine can effectively be reduced using a TLCD.

A pontoon-type platform was equipped with a TLCD mitigation system by Lee and co-workers (Lee et al. 2006). The amount of absorption through the TLCD was evaluated and corresponded to different diameters, masses, and drafts of the pontoon. According to this study`s analytical part, the amount of the dissipated energy through TLCD can reach a value higher than 70%. The amount of the dissipated energy also decreased from 73% to 55% due to the increase in the pontoon`s dimension. When the pontoon draft is increased the mitigating effect of TLCD is decreased from 55% to 46% which also shows that increasing pontoon dimensions negatively affect the absorption of TLCDs. It is also concluded that besides motion mitigation, TLCDs could be effective in vibration suppression for floating platforms (Lee et al. 2006) since the results show that when the platform is subjected to high-frequency excitations, especially between 5 Hz and 6 Hz pitch response in rotation, can be effectively suppressed by TLCD.

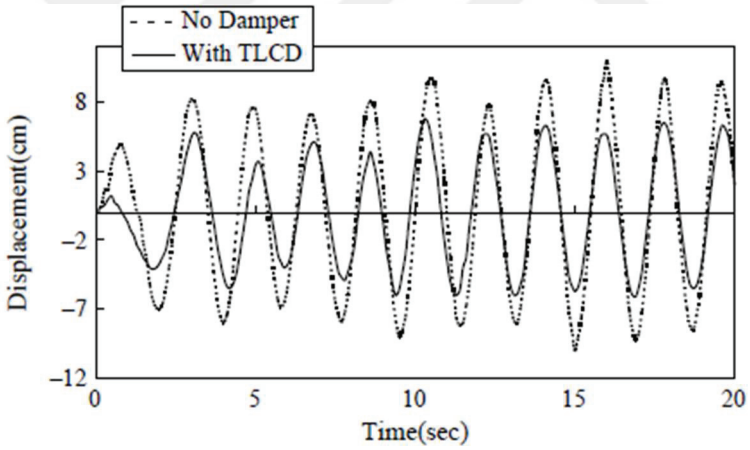

Figure 1.2 Displacement time story of a Tension Leg Floating Platform with and without TLCD damper. (Source: H.H. Lee et al. 2006)

Motion mitigation of a structure is also important for extending its lifespan considering fatigue. A multi-degree of freedom of offshore wind turbine movements is investigated under wind and wave excitations in a numerical study by Colwell and Basu (2009). According to this study, the structure`s peak response of offshore wind turbines that are subjected to wind and wave is down up to 55% when TLCD is equipped (Colwell et al. 2009). The cumulative fatigue damage rate per year is also decreased from 0.0017 to 0.00014 by using TLCD on top of the mono-pile foundation.

In another research, a tension leg type floating platform was incorporated with a TLCD located inside of the floating platform where its maximum responses were measured experimentally in which the average reduction of the surge motion was obtained as 25%, the maximum amplitude reduction of the surge motion was measured as 30%. Heave motion reduction was also measured up to 16% while the heave response of the platform was amplified as little by underwater TLCD for 6cm wave height condition. Mitigation ratios of pitch motion were observed to be better than surge and heave. According to the experiment results, pitch motion was reduced by up to 50%. Another interesting finding was that, when the amount of liquid employed in the columns is increased there was less reduction effect in the heave Lee (Lee et al. 2012) which shows that there must be an optimum liquid amount that maximizes the heave mitigation.

An experimental study was performed by Jaksic and co-workers (Jaksic et al. 2015) to show the benefits of using TLCD in model tensions leg floating platform. Three different TLCDs (as shown in Figure 1.3) were used to control the motion of the platform. The effect of the combination of these dampers was also experimentally monitored where the effect of the mass ratios of the TLCDs was observed. The maximum reduction in surge motion was 16%, while three TLCDs were activated with a 10% mass ratio.

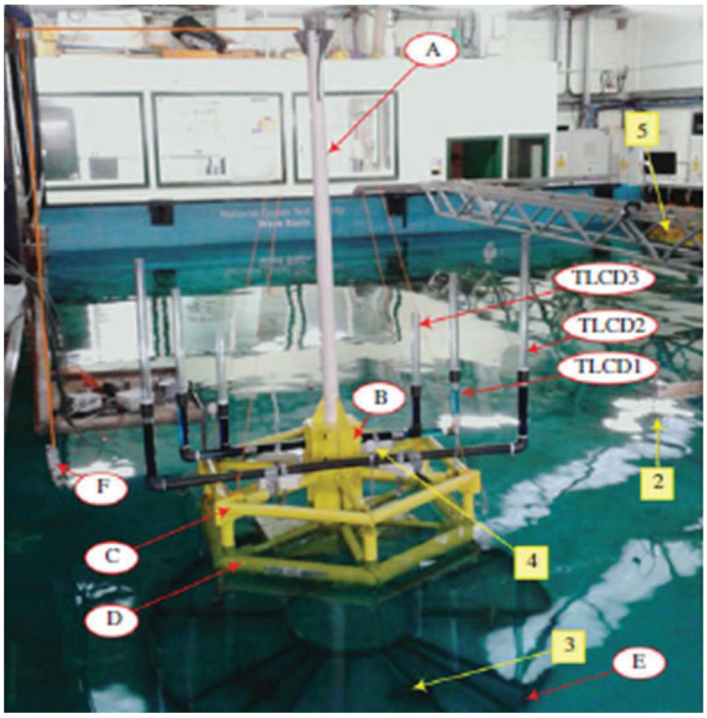

Figure 1.3 50 scale Tension Leg Platform and three different TLCDs.
(Source: V. Jaksic et al. 2015)

Dynamic analysis and natural frequency of structure were performed using MATLAB in another study by Hemmati (Hemmati et al. 2019). The natural frequency value of the structure was also verified with results from previous fundamentally different computational fluid dynamic studies. Studies cover active and inactive TLCD systems, and fragility analysis of structure was also considered. According to the study, fragility reduction of the structure was observed up to 13% by controlling the dynamic response of the structure with TLCD. In addition, the standard deviation of the top-of-the-tower response was down up to 49% for an optimized TLCD. It was also noted that using TLCD the reduction of the fragility of the structure is higher for low-intensity earthquakes (Hemmati et al. 2019).

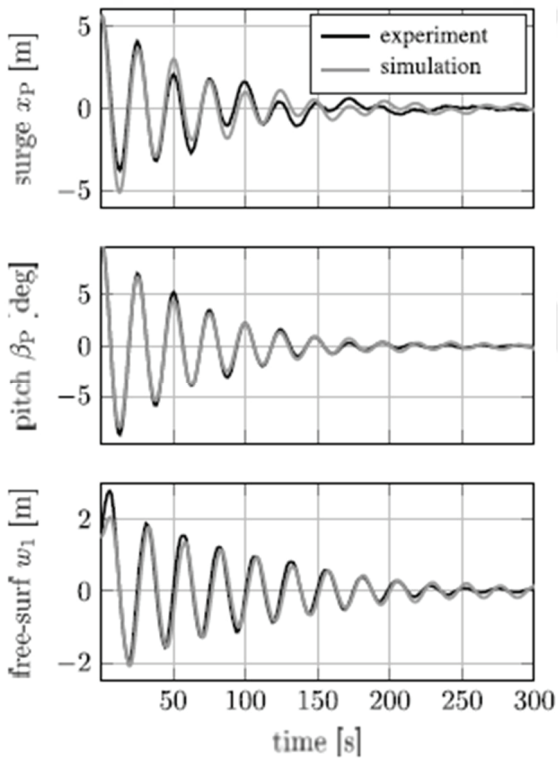

Figure 1.4 Comparison of time response between simulation and experimental results. (Source: Wei Yu et al. 2023)

The mitigation of pitch motion of a semi-submersible floating offshore wind turbine was investigated by Xue (Xue et al. 2022) using TMLCD. According to this study, the pitch response of the structure was reduced by 10.84% to 18.53% under resonance frequency while the mass ratio was equal to 2%. When frequency ratios are equal to 0.8,

1.0, and 1.1 the damping effects of the TLMCD are 71.97%, 97.29%, and 82.63% respectively Xue (Xue et al. 2022).

An experimental and numerical study on the stabilizing effect of a TLMCD on floating wind turbines was done by Yu (Yu et al. 2023). Root mean square error of experimental and numerical results were obtained for two different load cases which were high wind speed condition, rotor speed, and blade pitch angle added.

According to this study, it was observed that there was a reduction in the surge and the pitch motions however an increase was observed in the heave motion when TLMCD was employed. The degree reduction of the surge was 36.7% and 16.6% for two load conditions. Whereas the reduction in pitch motion of the structure was 17.7% and 14.4% radians for two load conditions. Despite the reduction of surge and pitch motions, the heave motion of the structure increases by 4.2% and 10.1% respectively for both conditions (Yu et al. 2023).

The direction of external excitations that are not always aligned with the absorber should also be considered. To absorb a non-aligned excitation, a single U-shape TLCD cannot be effective. Two U-shape TLCDs that are perpendicular to each other offer the possibility to absorb the non-aligned excitation more effectively. Three columns of TLMCDs are shown to be used effectively to reduce non-aligned excitations. Coudurier (Cuodurier et al. 2018) showed that using three-legged TLMCDs is more effective than using two perpendicular TLCDs.

1.4.4 Orifice Effect on Damping Performance of TLCD

Damping of a TLCD is principally produced by an orifice which causes a head loss when liquid moves through the orifice harmonically inside the column. The absorption performance of the TLCD is directly proportional to the head loss coefficient of the U-shape. Therefore, an optimum and adaptable absorption can be provided, which means that the head loss coefficient of the TLCDs should be tuned concerning excitation`s amplitude or frequency with structure specifications to obtain the best mitigation response. Yalla and co-workers (Yalla et al. 2000) concluded that determining the optimum head loss coefficient that is adjusted by controlling the orifice opening ratio of a TLCD is related to the damping of the primary structure.

La and Adam (La et al. 2018) applied an on-off damping controller that provides two different head loss coefficient values ten times greater than the passive head loss

coefficient value. According to the study`s result when on-off damping control is activated, the peak displacement of the four-storey structure was 23.4 cm compared to the passively controlled structure with 29.8 cm. Altay and Klinkel (Altay et al. 2018) performed a series of experiments on semi-active TLCD, which provides different head loss coefficient values through movable butterfly valves which are in the middle the of horizontal column to adjust the blocked area. Damping ratios of a TLCD were obtained by adjusting panel position for three different angles at 45°, 58°, and 72° (with constant valve position fully open at 90°). The highest damping ratio was determined for 45° as 6.5% the lowest damping ratio at 72° was 4.8% (Altay et al. 2018). Yalla and co-workers (Yalla et al. 2001) concluded that a semi-active TLCD provides better response reduction than passive TLCD for harmonic and random excitations by adjusting the opening ratio of the orifice through a valve. They also noted that, after a critical head loss coefficient value, improvement of response reduction was minor (Yalla et al. 2001). Wu (Wu et al. 2005) also formulated a relation between the orifice blocking ratio and the head loss coefficient of a TLCD and concluded that while the blocking ratio of an orifice increases, the head loss coefficient of TLCDs increases.

1.5 Motivation

A passive TLCD will be examined that is subjected to different external excitation conditions to investigate the effect of the head loss coefficient on damping performance of the TLCDs. The head loss coefficient of liquid column dampers can be varied using orifices or any type of frictional factor. In general, the damping capability of liquid column dampers is produced using an orifice that is in the middle of the U-shape TLCD. Due to this orifice liquid column dampers have an almost constant head loss value. Using more orifices which are located inside the liquid column different head losses and damping values were proposed to be obtained with respect to different external excitation values. As mentioned above in previous studies, if the head loss coefficient of a TLCD can be adjusted concerning excitation conditions, the damping performance of TLCD will be improved. When many orifices are located inside the U-shape TLCD, it can be expected that the amount of head loss can be varied concerning the liquid column oscillation amplitude and velocity, which are also dependent on structure movement.

In this thesis, the positive effects of extra orifices will be monitored to minimize the disadvantages of using only one orifice therefore, the damping effect of a passive

TLCD will be improved by adjusting the head loss coefficient through these extra orifices. Analytical model analysis and a series of experimental investigations will be completed for these dampers to observe the effects of using extra orifices on the damping performance of the U-shape TLCDs.

CHAPTER 2

ANALYTICAL AND NUMERICAL METHODOLOGY

The general form of the equation of motion will be rearranged for a U-shape TLCD to determine the mass, damping, and stiffness values of a liquid column. All these magnitudes will be derived, and the relationship between damping and head loss coefficient of the TLCD will be comprehensively examined. The effect of the orifice blocking ratio on the head loss coefficient will also be investigated. Responses of TLCD and primary structure can be simultaneously obtained by solving these differential equations for harmonic or random excitations.

2.1 Determining Equation of Motion for Linear Damped Single Degree of Freedom System

Under this title, an equation of motion expression will be obtained for a damped single-degree-of-freedom system that oscillates harmonically. When any object that is attached with a stiffness and a damper oscillates under any harmonic excitation or concerning any initial conditions such as displacement, velocity, or acceleration, motion plots can be obtained using the equation of motion. A schematic demonstration and free-body diagram of a single-degree-of-freedom system is shown in Figure 1.

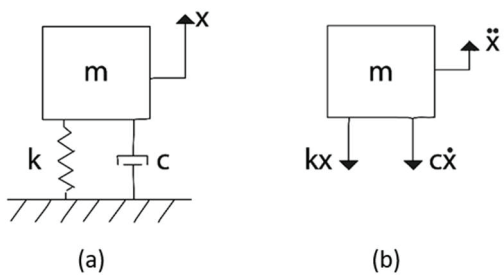

Figure 2.1 DOF (a) A single degree of freedom system, (b) and free body diagram.

According to, Newton`s second law of motion amount of momentum changing with respect to the time of any mass is proportional to changing of force that acts on it as shown in Equation 2.1.

$$\sum F = \frac{d}{dt}(mv) = m\frac{d}{dt}\left(\frac{dx}{dt}\right) \tag{2.1}$$

where, F is force and m is mass, v is velocity and x is the location of mass. The second derivation of x is also equal to the acceleration of mass. This expression is also shown in the following equation.

$$\sum F = m\frac{d^2x}{dt^2} = m\ddot{x} \tag{2.2}$$

where, is equal to the acceleration value of mass. The mass of the single-degree-of-freedom system is exposed to stiffness and damping force with external force as shown in Figure 1. These forces can be expressed in Newton`s second law of motion at the left-hand side of the equation.

$$F(t) - F_k(t) - F_c(t) = m\ddot{x} \tag{2.3}$$

where, F(t), $F_k(t)$, and $F_c(t)$ are equal to external force, stiffness force, and damping force respectively. Stiffness force and damping force are proportional to displacement and velocity of mass respectively. The final form of this equation also called equations of motion is shown in Equation 2.4.

$$m\ddot{x} + c\dot{x} + kx = F(t) \tag{2.4}$$

where, c and k are the damping and stiffness coefficient of the damped single Degree of freedom system, respectively. In this equation, the external force F(t) can be defined as any harmonic function. The equation of motion is a differential function that is second-order, linear, and inhomogeneous. However, this function can also be solved as homogenous without any external force. Dynamic response of mass can be calculated as displacement, velocity, and acceleration stories with respect to time using the equation of motion. While displacement, velocity, and acceleration values are obtained, these motions can be plotted with respect to the equilibrium position of the mass. This form of the equation of motion is a general expression of damped single-degree-of-freedom objects,

which are exposed stiffness and damping force with any applied external force like a harmonic force function.

In this equation, damping coefficient c and stiffness coefficient k are constant values however, the amount of the damping and stiffness forces change with respect to mass motion. The frequency of the oscillation motion of mass and damping ratio of the single Degree of freedom system are also dependent on mass and both damping and stiffness coefficient. The natural frequency and damping ratio of the system are calculated using these parameters.

$$\omega = \sqrt{\frac{k}{m}} \tag{2.5}$$

$$\zeta = \frac{c}{c_{cr}} = \frac{c}{2\sqrt{km}} \tag{2.6}$$

where, ω is equal to the natural frequency of system oscillation. ζ and c_{cr} are called damping ratio and maximum damping of the system respectively. Critical damping shows us the maximum damping value of the system. The damping ratio shows the ratio of the damping value produced in the cycle to the critical damping value. However, while the amount of damping produced in a cycle is equal to critical damping the oscillator returns equilibrium position as quickly as possible. During calculations, the damping ratio is used to define the damping performance of the system. All these above equations are used to calculate the response of the system as displacement, velocity, and acceleration.

2.2 Determining of Equation of Motion for TLCD

The traditional form of equation of motion was derived from Newton`s second law of motion as shown in Equation 2.4. This equation can be used to obtain motion data of damped single-degree-of-freedom systems while any external harmonic force or initial condition is applied to the system. In these systems, stiffness and damping coefficient values are already known. However, stiffness and damping values are inherently produced in TLCDs. These values are calculated in terms of column specifications such as density of liquid, diameter, and length of column, or head loss term.

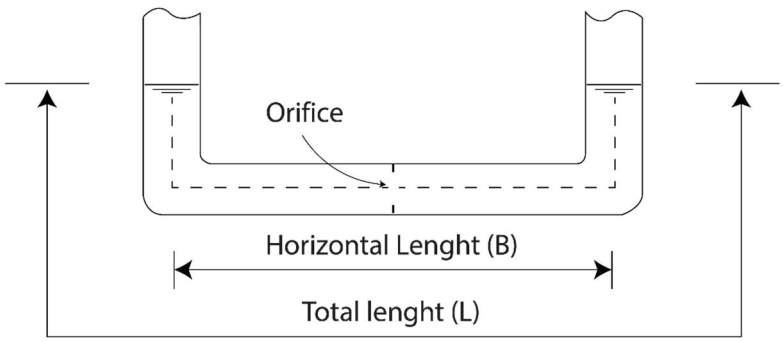

Figure 2.2 A U-Shape TLCD.

If any U-shape tuned liquid column dampers are designed as shown in Figure 2.2, mass, stiffness, and damping terms of the equation of motion can be calculated as follows.

$$\rho AL\ddot{x} + \frac{1}{2}\rho A\eta|\dot{x}|\dot{x} + 2\rho Agx = F \tag{2.7}$$

where, ρ, A, L, and g are the density of the liquid, the cross-sectional area of the column, the total length of the liquid column and the gravitational constant, respectively with B showing the horizontal distance in between vertical columns. The head loss coefficient term of η is also calculated using a fluid mechanics equation.

$\dot{x}$ and $\ddot{x}$ are first and second derivations of the surface elevation value of liquid with respect to time. F is defined as a harmonic force function which is applied to the column. However, the right-hand side of this equation can also be equal to zero to solve this equation as homogeneous to observe the decay behaviour of the liquid column. The mass of the liquid column is calculated using the equation of $m = \rho AL$. The amount of damping is also calculated using the damping equation of $c = \frac{1}{2}\rho A\eta|\dot{x}|$. The stiffness of liquid column is equal to the equation of $k = 2\rho Ag$. The natural frequency of TLCD can be calculated as shown in equation 2.8.

$$\sqrt{\frac{2g}{L}} \tag{2.8}$$

Due to the nonlinear behaviour of the damping term, the equation of motion of the tuned liquid column damper is not a linear differential equation. The absolute velocity

value of the liquid surface is proportional to the damping term. The nonlinearity of the equation of motion for TLCDs causes complexity in solving this equation analytically. The equivalent linear damping value of tuned liquid column dampers was calculated using the statistical linearization method by (Yalla et al. 2000). Linear expression of damping was also proposed as an equivalent form of the damping term while the liquid column is subjected to harmonic excitation (Wu et al. 2005). However, the equation of motion of liquid columns can be solved by applying appropriate numerical methods instead of damping term linearization.

2.3 Analytical Model Coupled Primary Structure and TLCD

Dampers are attached to structures to suppress the motion of the primary system by dissipating the motion energy of the system. Primary structure and tuned liquid column damper motions should be simultaneously calculated using the equation of motions of structure and damper. The schematic demonstration of the coupled primary structure and tuned liquid column damper system is shown in Figure 2.3.

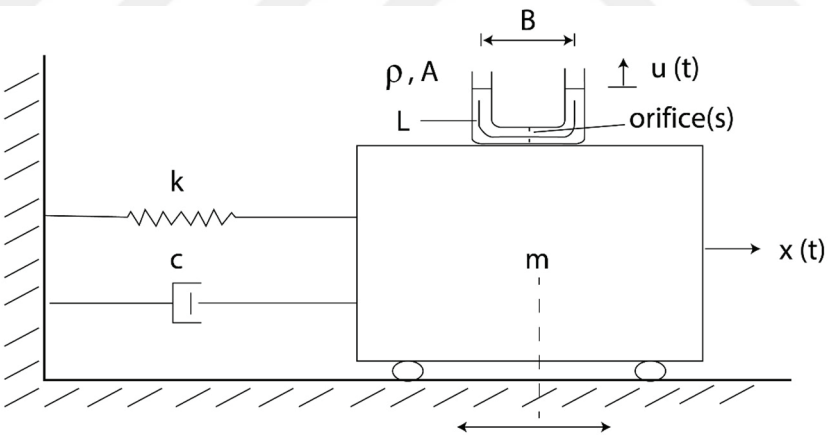

Figure 2.3. Analytical model of a coupled structure and absorber system TLCD is located.

M_s, C_s, and K_s show mass, damping and stiffness of the primary structure, respectively. X_s is equal to the displacement value of the primary structure with respect to time. Two equations of motions can be solved to calculate the response of both primary system and liquid surface motions. These coupled system responses are obtained by solving the below system of differential equations.

$$\begin{bmatrix} M_s + m_f & m_{fh} \\ m_{fh} & m_f \end{bmatrix} \begin{Bmatrix} \ddot{X}_s \\ \ddot{x}_f \end{Bmatrix} + \begin{bmatrix} C_s & 0 \\ 0 & c_f \end{bmatrix} \begin{Bmatrix} \dot{X}_s \\ \dot{x}_f \end{Bmatrix} + \begin{bmatrix} K_s & 0 \\ 0 & k_f \end{bmatrix} \begin{Bmatrix} X_s \\ x_f \end{Bmatrix} = \begin{Bmatrix} F \\ 0 \end{Bmatrix} \tag{2.9}$$

Nonlinear damping term and stiffness value of liquid column are applied to a system of differential equations where,

$$c_f = \frac{1}{2}\rho A\eta\left|\dot{x}_f\right| \tag{2.10}$$

$$k_f = 2\rho A g \tag{2.11}$$

The last form of the coupled system equations is shown in Equation 2.12 with adding Equation 2.10 and 2.11 to Equation 2.9 below.

$$\begin{bmatrix} M_s + m_f & m_{fh} \\ m_{fh} & m_f \end{bmatrix} \begin{Bmatrix} \ddot{X}_s \\ \ddot{x}_f \end{Bmatrix} + \begin{bmatrix} C_s & 0 \\ 0 & \frac{1}{2}\rho A\eta\left|\dot{x}_f\right| \end{bmatrix} \begin{Bmatrix} \dot{X}_s \\ \dot{x}_f \end{Bmatrix} + \begin{bmatrix} K_s & 0 \\ 0 & 2\rho A g \end{bmatrix} \begin{Bmatrix} X_s \\ x_f \end{Bmatrix} = \begin{Bmatrix} F \\ 0 \end{Bmatrix} \tag{2.12}$$

Here, F can be any harmonic force function that is applied to the primary structure. This equation system can be solved for both cases either under external force or any initial condition value such as initial displacement of structure with respect to the equilibrium position of the primary structure. The total mass of the liquid column and the horizontal part of the liquid mass are symbolized as m_f and m_{fh}, respectively.

These equations should be solved numerically due to the nonlinear damping term of TLCD. Numerical integration provides a means of solving the equation of motion of a damped single-degree-of-freedom system oscillator without solving second-order differential equations in closed forms. This numerical method can be applied to simultaneously solve the equation of motion of both the primary structure and liquid column. Nonlinear damping term can be obtained using liquid surface velocity value for each step without applying a linearization method during numerical calculations.

This numerical method is applied to equations of motion to obtain displacement, velocity, and acceleration values of a single Degree of freedom system. Equation 2.4 can be arranged for given an increment value and mechanical properties of the system as follows,

$$m\left(u_{n+1} - u_n - \dot{u}_n h - \ddot{u}_n \frac{h^2}{3}\right)\frac{6}{h^2} +$$

$$c\left[(u_{n+1} - u_n)\frac{3}{h} - 2\dot{u}_n - \ddot{u}_n \frac{h}{2}\right] + ku_{n+1} = F_{n+1} \tag{2.13}$$

where, h is equal to the increment value and $u, \dot{u}, and\ \ddot{u}$ are displacement, velocity, and acceleration value of a single Degree of freedom system, respectively (n=0,1, 2, 3, ….).

Equation 2.12 can be rewritten as a form of the numerical approximation, which is formulated in Equation 2.13. In this formulation, the nonlinear damping term can be calculated as a numerical for each step. Thus, the amount of damping can be obtained that is more accurate for each step of numerical calculation instead of using an equivalent damping term.

```
Input: Initial parameter (displacement), increment value, analyse duration
Define time as 0
Define results as an empty list
while time ¡ duration do
    Calculate displacement, velocity, and acceleration values
    values ← CalculateValues(displacement)
    displacement, velocity, acceleration ← values
    Calculate nonlinear damping value
    nonlinear_damping ← CalculateNonlinearDamping(velocity)
    Save calculation results
    Append (time, displacement, velocity, acceleration,
    nonlinear_damping) to results
    Increment time by the increment value
    Update displacement by the increment value
end while
Export calculation results as displacement, velocity, and acceleration values
with respect to time
```

Figure 2.4 Algorithm for the solution of analytical model.

In structural dynamics calculations, the increment value can be selected as 5% of the period value while the numerical calculation is obtained. Even if the lower increment values were applied, the results of the damping ratio calculations could not be affected as well. This numerical approximation was coded with given algorithm in Figure 2.4 in Python, as shown in Appendix C.

2.4 Head Loss Coefficient and Orifice of TLCDs

When fluid flows inside a column, the kinetic energy of the liquid is dissipated through an orifice that is generally located in the middle of the horizontal part of the column. Due to its viscosity, liquid kinetic energy is consumed by frictional effects. Moreover, the opening ratio of the orifice is directly related to the amount of the consumed liquid energy. This relation was investigated for steady flow in pipe and an empirical equation was formalized in Idelchik`s Handbook of Hydraulic Resistance (Idelchik 2008).

The liquid is discharged through a sharp-edged orifice; the resistance coefficient can be calculated by the following equation.

$$\eta = \left(1 + 0.707\sqrt{\beta}\right)^2 (1-\beta)^{-2} \tag{2.14}$$

Here, β (opening ratio) shows the area ratio of the cross-sectional grid to orifice. As shown in Idelchik formulization (Equation 2.14), the head loss coefficient of flow can be calculated using only the orifice opening ratio. This relation was also rearranged for tuned liquid column dampers by applying a series of forced harmonic vibration experiments by Wu and co-workers (Wu et al. 2005). They obtained a modified form of the head loss coefficient equation with respect to opening ratio which is presented in Equation 2.15.

$$\eta = (-0.6(1-\beta) + 2.1(1-\beta)^{0.1})^{1.6}(\beta)^{-2} \tag{2.15}$$

These approaches can be used to calculate the head loss coefficient as formulated in Equations 2.14 and 2.15. However, when the opening ratio of the orifice is higher than 0.3, these equations give nearer results as shown in Figure 2.5. While the opening ratio decreases, differences between the values of these two equations increase.

As shown in previous studies, the head loss coefficient of tuned liquid columns can be calculated using the equation by Wu (Wu et al. 2005) under harmonic excitations. As shown in the equation, the orifice blocking ratio is the only parameter that is used to calculate the head loss coefficient.

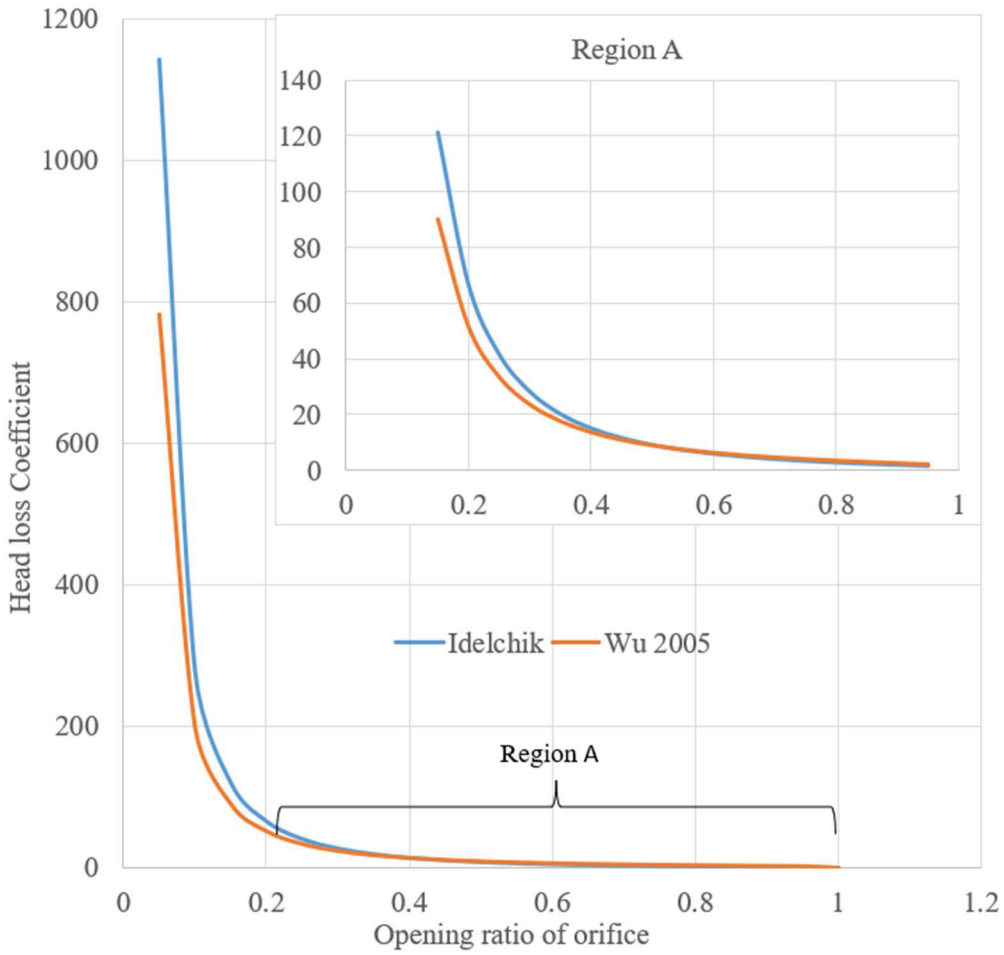

Figure 2.5 Head loss coefficient calculation with respect to opening ratio of cross-section.

CHAPTER 3

EXPERIMENTAL METHODOLOGY

Due to the nonlinear damping term of a TLCD`s equations of motion and the complexity of determining the head loss coefficient of an orifice, coupled primary structure and TLCD system responses can only be obtained by solving these equations numerically. Even if equations of motion for both structure and liquid-free surface can be solved numerically, the head loss coefficient value should also be supported by applying a series of decay experiments. Response-time stories of experimental design can also be used to verify the numerical calculations. During these experiments, structure response were observed using video and analysed afterward (by free distribution Tracker software). Modeling tools which are measuring, calibration, and coordinating were used to obtain time series plots of the top point of the structure, located on the U-shape TLCD.

The objective of this study is to observe the impact of spacing between orifices on damping performance, so other effects are not considered during this research like scaling, viscosity, density of liquid, and structure features.

3.1 Experimental Design

According to analytical methodology requirements, experimental design is mainly separated into two parts corresponding to the physical features of the structure and damper. A wooden structure was constructed to simulate a primary structure whose motions are suppressed by employing a U-shape TLCD made of polylactic acid (polymer PLA) by a three-dimensional printer. Geometry of this TLCD is shown in Figure 3.2 below. Experimental setup visual is also shown at the end of Chapter 3 in Figure 3.4.

A video recorder device is used to capture structure motion in 30 fps (frames per second). Thereafter, time series of the motion (displacement) of the structure is obtained by a motion tracker software (Source: Open-Source Physics designed for use in physics education and hosted by the AAPT-ComPADRE Digital Library). Physical properties of structure such as natural frequency, stiffness, and damping ratio are obtained by analysing the motions through Tracker software as shown in Appendix B.

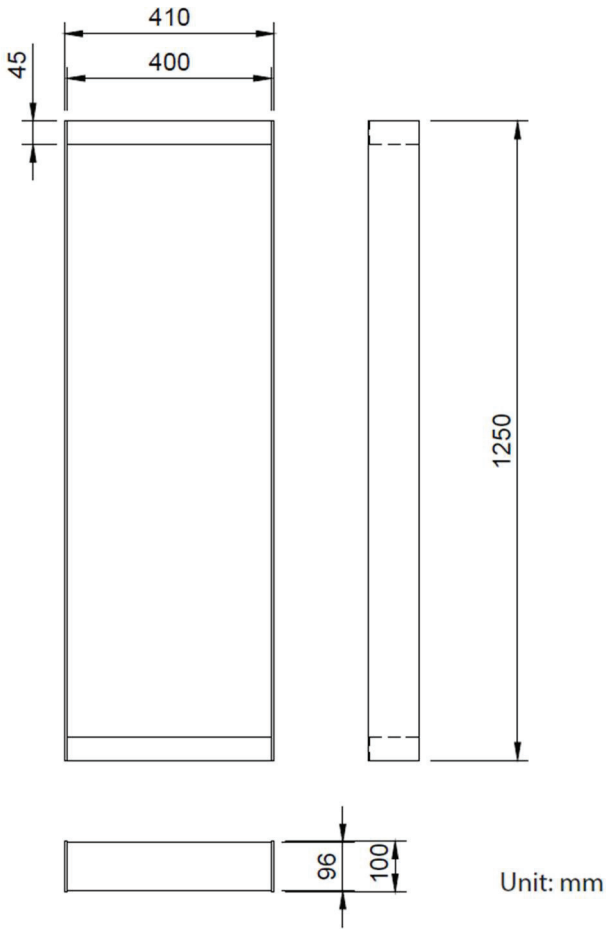

Figure 3.1 Technical Drawing of the Structure.

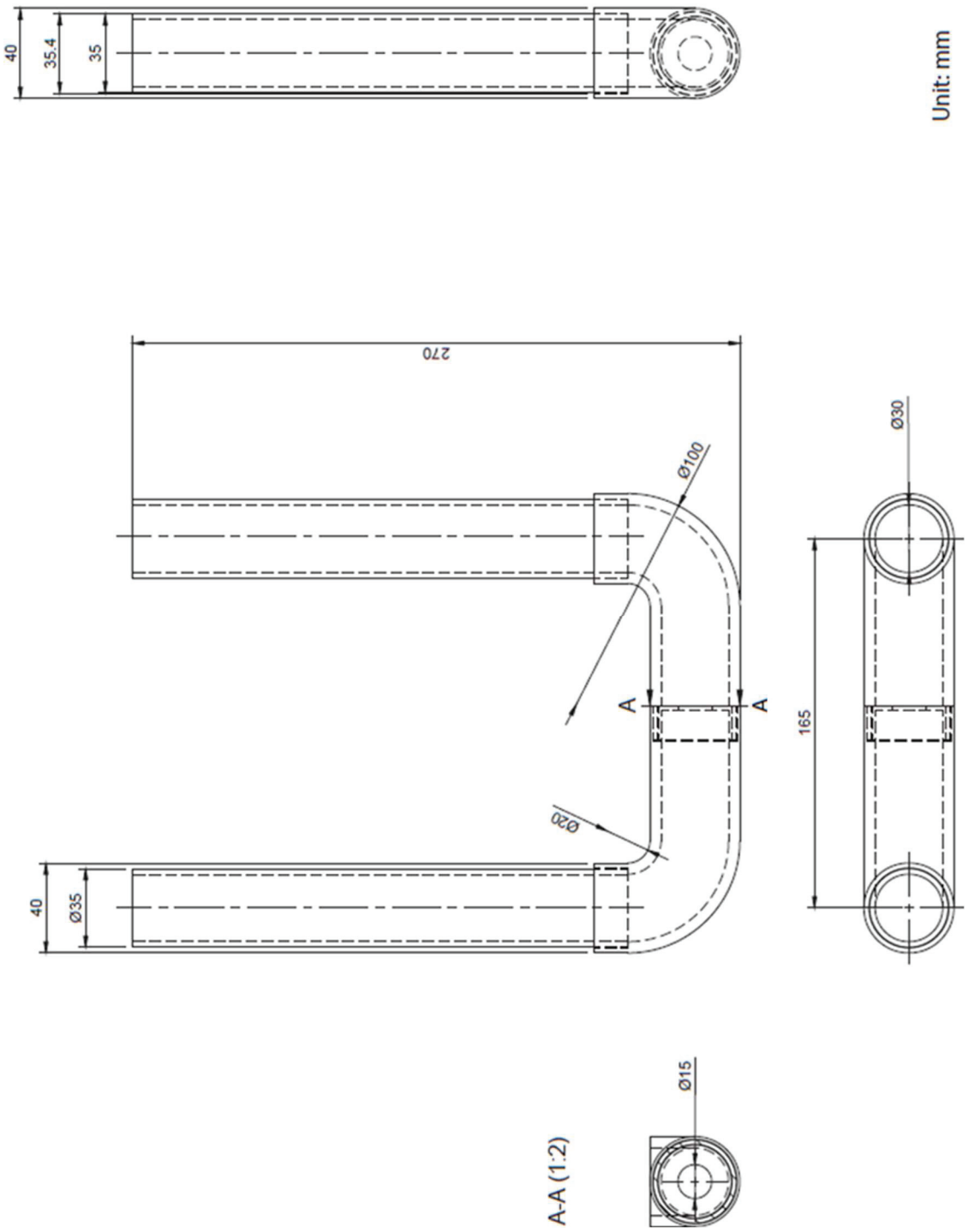

Figure 3.2 Technical Drawing of the U-Shape TLCD.

3.2 Explanation of Experimental Process and Data Collection

In structural analysis, structure or damper responses are monitored under external excitations by considering the mechanical features of the coupled system, such as frequency, stiffness, and damping. When a building is subjected to any type of external force, the response of the building is varied due to many parameters such as frequency or amplitude of force or location of force applied. Response of structures can be determined for any location of buildings by knowing exactly applied force parameters with location and direction. Using mechanical features of structure and damper all structural responses can be calculated if external excitation conditions are known therefore absorption performance of the damping system is also determined.

Decay tests can be effectively used to obtain both structure and damper specifications by observing the decrement values of each periodic motion. During a decay experiment an initial condition is defined and applied to the structure such as displacement, velocity, or acceleration. Then displacement-time series are obtained; therefore, the damping ratios and damping values of each cycle and the natural frequency of systems are obtained. When a structure or a damper is subjected to harmonic excitations, the response of it can also be calculated if external force frequency and amplitude are known with the location where the force is applied. Mechanical properties of structure and TLCD will be obtained by applying a series of decay experiments, and their responses are recorded by a video camera and motion time-series are obtained by Tracker video software. Analysing these displacement time series resulted in its damping, stiffness coefficients. Using video analysis provides the advantages such as putting aside the usage of sensors in determining structure frequency and, not adding extra mass that affects the natural frequency of structures. However, an electric motor with a centrifugal mass can also be used to oscillate the structure harmonically; in this case mass of these extra elements should be considered in determining properties of structures and U-shape TLCDs. Therefore, such as a perturbation system is only used if its mass considerably smaller than the structure`s.

As mentioned in previous sections, the results of experiments that will be used to support the results of the analytical model, which does not include some of the encounterable effects in real life, such as drag of air or thermal environment conditions, should be purified from all extra facts.

3.3 Determining Physical Properties of Structure and TLCD with Experiment

To obtain the stiffness, natural frequency, and damping value of the structure with or without a TLCD damper, a series of experiments are employed. During experiments, the top of the structure's initial displacement is defined as the distance value with respect to the ground then the structure is released, and motions are observed while TLCD is active or inactive. All these experiments and their results are investigated and compared concerning tuning ratio which is defined as the natural frequency ratios of the structure to the damper.

Firstly, the natural frequency of the structure is obtained by observing a series of decay experiments under different conditions while changing the mass of the structure. A typical displacement time series obtained from one of these experiments is given in Figure 3.3. Investigating these experiment's results, the natural frequency of structure can be accurately obtained by using these displacement time series plots. During structure oscillating 23 peaks occur 13.9 seconds which means the natural frequency of structure is 10.3966 rad/s. Due to the fps quality of the videos, the accuracy of results is between ±0.2 rad/s. Using the natural frequency of structure stiffness, mass, damping ratio, and damping value can be calculated. Physical specifications of the structure were obtained by applying two decay experiments and these results were noted in Table 3.1 below.

Table 3.1 Structure mechanical specifications and their values.

Physical Specifications of Structure				
Natural Frequency ω (rad/s)	Mass m (kg)	Damping C (Ns/m)	Stiffness K (N/m)	Damping Ratio 5 cycles ζ (-)
10.3675	0.728	0.26	78.25	0.01725

The physical specifications of TLCD can be calculated by using the parameters of TLCD geometry as mass, damping, and stiffness. The mass of the U-shape should also be considered during the experiments and the analytical model calculations. The natural frequency of the TLCD is only related to the length of the liquid column as shown in Equation 2.8. The mass of the liquid column is calculated with the geometrical properties of a U-shape, or it can be weighing.

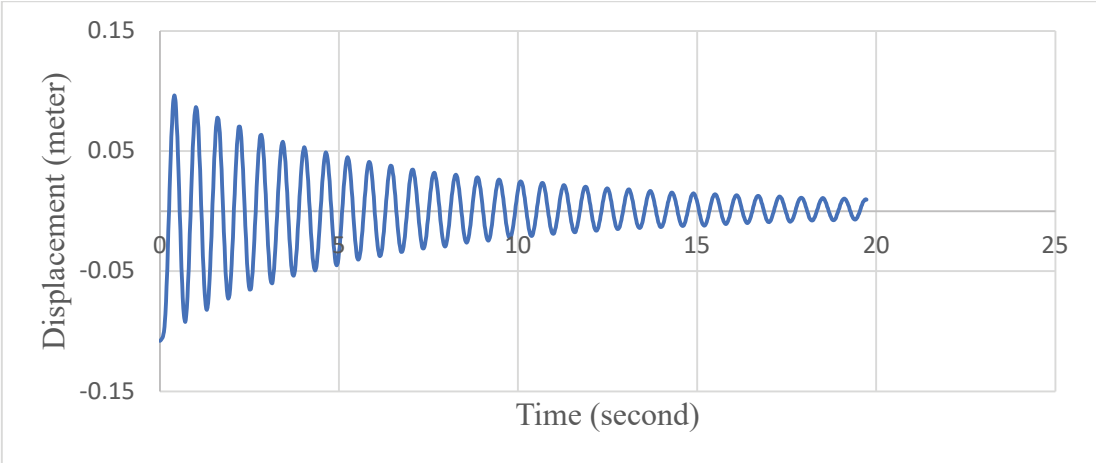

Figure 3.3 Structure displacement-time story without damper.

The stiffness of the TLCD is a function of the density of the liquid, the cross-sectional area of the U-shape, and gravity as shown in Equation 2.11. The nonlinear damping term is a significant part of the damping capability of the TLCDs. Due to the nonlinearity, the velocity term of the liquid inside of the column is proportional to the amount of the damping term in the equation of motion. When the amount of the damping is calculated the head loss term of flow should also be considered. The head loss is a result of the frictional force to which liquid is exposed during flow inside of the U-shape TLCD. Experimental results are investigated to obtain the head loss term of the flow. In this thesis, the head loss of the flows was obtained by observing decay experiments which were investigated using a video modeling tool. Physical properties of the U-shape TLCD are noted in the Table 3.2 below.

Table 3.2 Mechanical properties of TLCD.

Physical Specifications of TLCD		
Natural Frequency ω (rad/s)	Liquid Mass m (kg)	Stiffness K (N/m)
7.9	0.222±0.001	13.868

The natural frequency of the structure changes due to the extra mass when the TLCD with liquid is located at the top of the structure. When the total mass of the U-shape TLCD and liquid column is equal to 0.419kg (0.222kg is weight of the liquid column and 0.197kg is weight of the TLCD), in this case the natural frequency of the coupled system would be 8.26 rad/sec. However, experiment results show that the

oscillation frequency of coupled system is approximately equal to 8.2±0.2 rad/s. In this case, the tunning ratio of the system which is defined as a natural frequencies ratio of the structure and the TLCD is approximately equal to 0.956 and 0.963 for analytical and experimental results respectively.

Figure 3.4 Visual of experimental setup.

CHAPTER 4

RESULTS

In this part, some of the investigations are presented which are obtained by using experimental and analytical models. The effect of the head loss coefficient on the stabilizing performance of TLCD is investigated to conclude the optimum head loss coefficient value.

Extra orifices were applied to the TLCD to change the head loss coefficient of the flow conditions in order to observe and compare the decay plots of the structure. When the number of the orifices is increased, the effect of the distance between extra orifices on the head loss coefficient is also monitored to observe the damping performance of the TLCD. When these decay experiments are performed by releasing the structure under different initial displacement conditions the effect of the head loss is monitored for each oscillation to observe the positive or negative damping effect of the head loss coefficient. While experimental results support the calculation of head loss coefficients, the numerical results of the analytical model are also used in calculating of nonlinear damping term of the TLCD. In much research, linearized terms are used to solve these problems, however, experiments and numerical solutions of analytical models can support each other in calculating these equations simultaneously.

4.1 Damping Performance of TLCD in Relation to Head Loss Coefficient

As mentioned in Chapter 2, TLCDs produce a head loss through the orifice which is in the middle of the U-shape. The amount of the head loss that is directly related to the opening ratio through an orifice which shows the resistance of the flow during the liquid column oscillation inside the U-shape. Many different head loss coefficients can be applied to the analytical model to check the effect of the head loss coefficient on the damping performance of the TLCD. This effect was also performed using experimental setup by adding extra orifices inside the column which are shown in Figure 4.2.

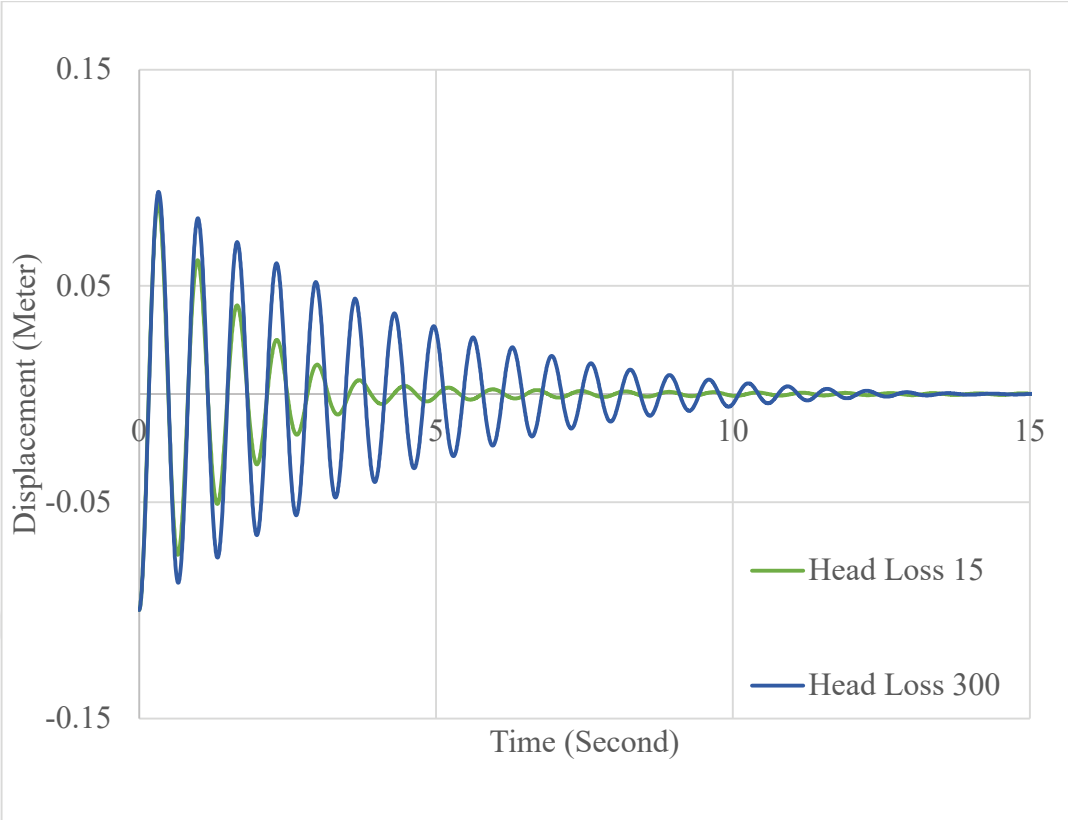

Figure 4.1 Decay plots of coupled system from analytical results with respect to different head loss coefficients.

The above plots demonstrate displacement time story of the structure where a TLCD is located when two different head loss coefficients are applied to the analytical model which is twenty times bigger than the other. As shown, when the head loss coefficient is equal to 15, the motion of the structure can quickly be decreased. However, if the head loss coefficient is equal to 300, the damping performance of the TLCD decreases which means that when the head loss coefficient increases the liquid column cannot move as quickly as to absorb the structure motions (as shown in Figure 4.1).

Table 4.1 Damping ratios of coupled system with respect to different head loss coefficients.

	Displacement for 5 cycles (meter)	
Time (Second)	Head Loss 300	Head Loss 15
0	-0.1	-0.1
3.31	-0.0478	-
3.45	-	-0.0097
Damping Ratios	0.024	0.074

The damping ratio values of these plots are also shown in Table 4.1 for the first 5 oscillations of the structure. Results show that the damping ratios of the first 5 cycles are equal to 2.4% for and 7.4% for head loss coefficients 300 and 15 respectively.

Experimental results also show that when the head loss coefficient is increased by applying extra orifices inside the liquid column which are shown in Figure 4.2, the damping performance of the TLCD and damping ratio of the oscillation plots decrease as shown in Figure 4.3. When three orifices are located inside of the U-shape TLCD, damping ratio of the oscillation plot was obtained as 2.5%. However, when only one orifice is active, the damping ratio of the oscillation plot was obtained as 4.1% for the first 5 cycles.

Figure 4.2 TLCD and extra orifices.

Technical drawing of the TLCD was presented in Figure 3.2 which demonstrates the fixed orifice in the middle of the column. Also, extra orifices can be located in horizontal part of the TLCD to observe the effect of extra orifices on damping performance of the system during experiments.

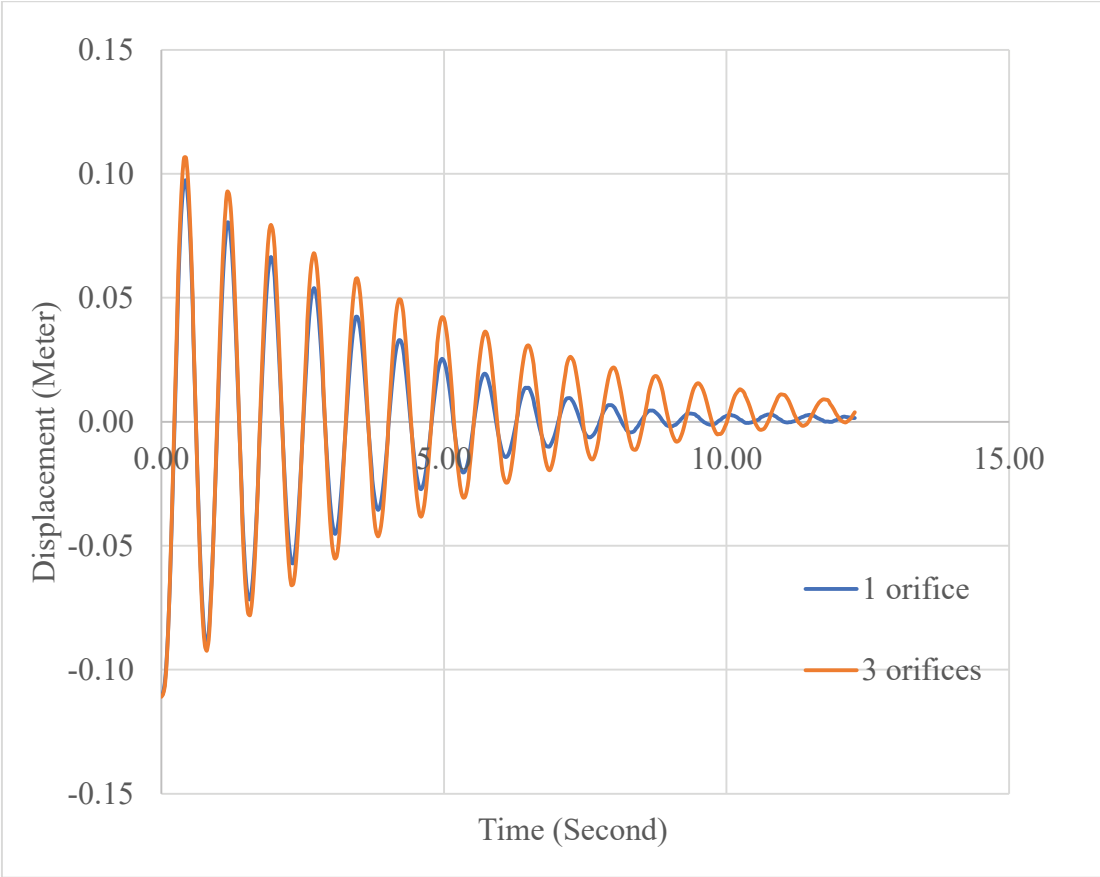

Figure 4.3 Decay plots of coupled system from experiment for one and three orifices.

Experimental and analytical results show that if the head loss coefficient is over the critical value, changing on damping performance of a TLCD is minor. Yalla and co-workers (Yalla et al. 2001) noted that after a given maximum head loss coefficient value, saturation is reached. There is a slight decrease in response after this critical value.

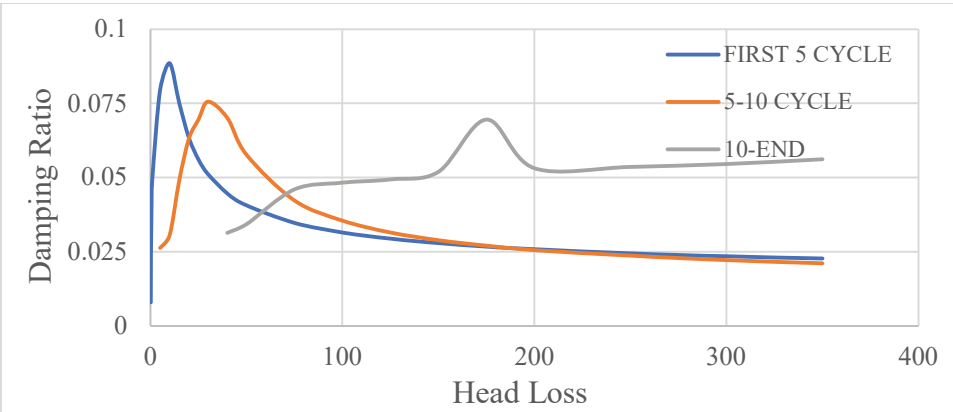

Figure 4.4 Damping ratios of coupled system with respect to different head loss values.

The optimum head loss coefficient values of different cycles are shown in Figure 4.4. These values were obtained analytically by solving the equations of motion by changing the head loss coefficient. Results show that lower head loss values are better for stabilization of structure at the start as shown in Figure 4.3. However, while the motion of the structure slows down optimum head loss coefficient value increases according to analytical model calculations as shown in Figure 4.4.

Yalla and co-workers (Yalla et al. 2003) noted that when the head loss value is adjusted through an actuator the structural movements can already be suppressed more effectively up to 15% - 25%. They also noted that constricting the liquid flow through the orifice at lower excitation amplitudes resulted in higher damping, while opening the orifice and increasing liquid velocity at higher amplitudes contributed to the proper amount of damping (Yalla et al. 2003).

However, while the liquid column oscillates through only one fixed orifice, the head loss values of the TLCD are almost constant in passive-absorbing systems. When the liquid column encounters one fixed orifice during oscillation, the orifice causes a resistance, due to the diameter reduction of the U-shape TLCD. Even if the number of orifices is increased, the head loss value of the TLCD is almost constant, when the distance between the orifices is not close to each other. However, if the distance between orifices is decreased head loss value of the column can change, even if the number of orifices is the same. The effect of the changing of the distance between orifices on the produced head loss value cannot be investigated analytically. It can be monitored by applying a series of experiments to investigate the effect of the distance between orifices on head loss value.

4.2 Experimental Investigation of the Effect of the Distance Between Orifices

When extra orifices are added to the system, their effect on head loss coefficient is not linearly additive, due to the fact that jet flow from one orifice affects the next one when are located in the proximity of each other. It was observed that while the number of the orifice is increased, the head loss value of the TLCD increases due to the extra orifices. However, the orifices inside the liquid column were located far away from each other the jet flow effect can be neglected.

A series of experiments were applied to check the effect of the distance between orifices on the head loss value. Distance between two orifices was adjusted as 0.5cm, 1cm, and 2cm to monitor its effect on the displacement at the top of the structure for the same decay experimental conditions. Decay plots of these experiments are shown in Figure 4.6 below. When the distance between two orifices is 0.5cm, the displacement-time plot shows that the motion of the structure was effectively absorbed by TLCD. However, when the distance between two orifices is increased the absorption performance of the TLCD decreases which also means that the head loss value of the TLCD increases while the distance between two orifices increases. Damping ratio values of these three plots are also compared in Figure 4.5.

Table 4.2 Damping ratio values with respect to distance between orifices.

A(meter)	B(meter)		
Orifice Diameter	Orifices Spacing	B/A	Damping Ratio
1.5	0.5	0.33333	0.029664
1.5	1	0.66667	0.028121
1.5	2	1.33333	0.026843

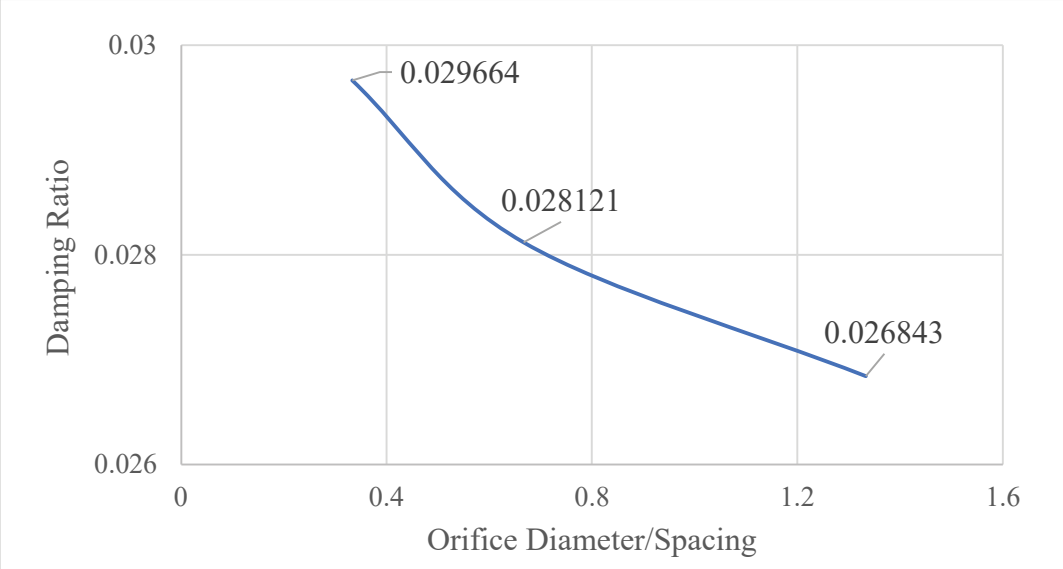

Figure 4.5 Damping ratio with respect to orifice diameter over orifice spacing.

Experimental results show that if two orifices are closer to each other the damping ratio of the coupled system increases, which means also that when orifices get closer to each other head loss value of the TLCD decreases.

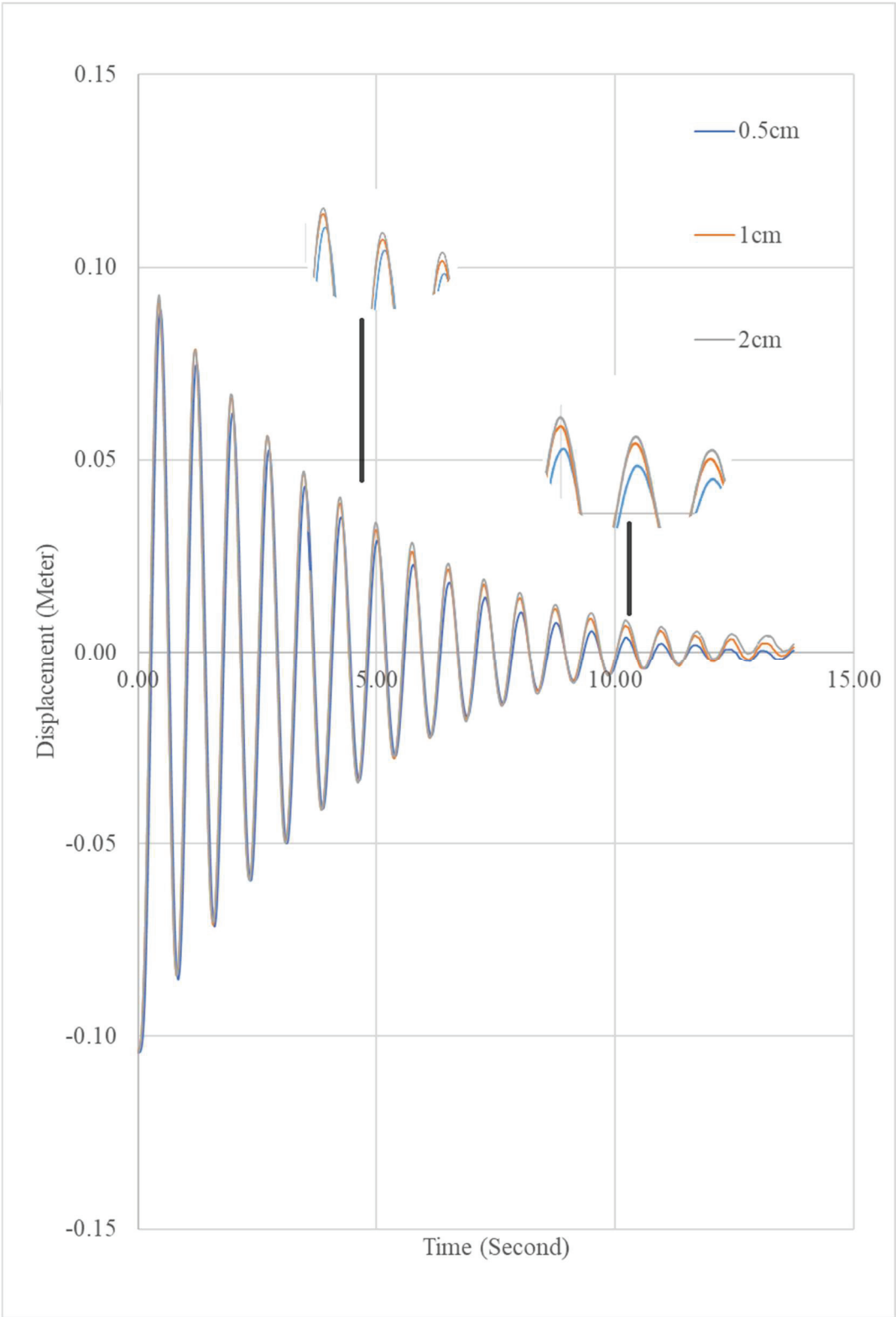

Figure 4.6 Decay plots of coupled system concerning distance between orifices.

CHAPTER 5

CONCLUSION

The objective of this thesis is to investigate the nonlinear behaviour of TLCDs by concerning the relation between the head loss coefficient and the damping performance of TLCDs. Equations of motion were solved for both structure and TLCD by applying a suitable numerical analysis approximation in Python. An experimental design was also prepared to monitor and check the coupled system displacement-time stories.

It was seen that structure oscillations can effectively be suppressed by using a U-shape TLCD for an optimized head loss value. However, if the head loss coefficient is over the optimized value, the damping performance of the TLCD will decrease according to both analytical and experimental results. The optimum head loss coefficient value cannot be calculated analytically due to the nonlinearity of the equation of motion; however, experimental investigations can be used to research the optimum head loss value.

The optimum head loss coefficient value is not the same for each cycle during the structure oscillating which is also the answer of why active TLCDs are designed. According to analytical model results, the optimum head loss value should be increased, when the amplitude of the structure oscillation decreases for better damping performance. It can be provided by adjusting the orifice diameter using an active TLCD system. It was also investigated that the distance between two orifices can be adjusted to obtain different head loss values. Thus, while the structure oscillates the damping performance of TLCDs can be improved as much as possible in all cycles. While the distance between orifices is changed, the damping coefficient value reached from 0.026843 to 0.02966, which means that the damping performance of the system was improved by 10.5%.

Using more orifices instead of only one can be proposed for the effective suppression of structural movements by U-shape TLCDs by adjusting space between orifices.

REFERENCES

Altay, Okyay, and Sven Klinkel. 2018. “A Semi-active Tuned Liquid Column Damper for Lateral Vibration Control of High-rise Structures: Theory and Experimental Verification”. *Structural Control and Health Monitoring*, 25 (12): e2270. https://doi.org/10.1002/stc.2270

Colwell, Shane, and Biswajit Basu. 2009. “Tuned Liquid Column Dampers in Offshore Wind Turbines for Structural Control”. *Engineering Structures*, 31 (2): 358-368. https://doi.org/10.1016/j.engstruct.2008.09.001

Coudurier, Christophe, Olivier Lepreux, and Nicolas Petit. 2018. “Modelling of a Tuned Liquid Multi-Column Damper. Application to Floating Wind Turbine for Improved Robustness Against Wave Incidence”. *Ocean Engineering*, 165*:* 277-292. https://doi.org/10.1016/j.oceaneng.2018.03.033

Idelchik, Isaac E. "Handbook of Hydraulic Resistance, Revised and Augmented." (2008).

Hemmati, Arash, Erkan Oterkus, and Nigel Barltrop. 2019. “Fragility Reduction of Offshore Wind Turbines Using Tuned Liquid Column Dampers”. *Soil Dynamics and Earthquake Engineering*, 125: 105705. https://doi.org/10.1016/j.soildyn.2019.105705

Jaksic, Vesna, C. S. Wright, J. Murphy, C. Afeef, S. F. Ali, D. P. Mandic, and V. Pakrashi. 2015. “Dynamic Response Mitigation of Floating Wind Turbine Platforms Using Tuned Liquid Column Dampers”. *Philosophical Transactions of the Royal Society A: Mathematical, Physical and Engineering Sciences*, 373 (2035): 20140079. https://doi.org/10.1098/rsta.2014.0079

La, Viet Duc, and Christoph Adam. 2018. “General on-off Damping Controller for Semi-active Tuned Liquid Column Damper”. *Journal of Vibration and Control*, 24 (23): 5487-5501. https://doi.org/10.1177/1077546316648080

Lackner, Matthew A., and Mario A. Rotea. 2011. “Structural Control of Floating Wind Turbines”. *Mechatronics*, 21 (4): 704-719. https://doi.org/10.1016/j.mechatronics.2010.11.007

Lee, Hsien Hua, and H. H. Juang. 2012. “Experimental Study on the Vibration Mitigation of Offshore Tension Leg Platform System with UWTLCD”. *Smart Structures and Systems*, 9 (1): 71-104. https://doi.org/10.12989/sss.2012.9.1.071

Lee, Hsien H., S-H. Wong, and R-S. Lee. 2006. “Response Mitigation on the Offshore Floating Platform System with Tuned Liquid Column Damper”. *Ocean Engineering*, 33 (8-9): 1118-1142. https://doi.org/10.1016/j.oceaneng.2005.06.008

Sadek, Fahim, Bijan Mohraz, Andrew W. Taylor, and Riley M. Chung. 1997. “A Method of Estimating the Parameters of Tuned Mass Dampers for Seismic Applications”. *Earthquake Engineering & Structural Dynamics*, 26 (6): 617-635.

Stewart, Gordon, and Matthew Lackner. 2013. “Offshore Wind Turbine Load Reduction Employing Optimal Passive Tuned Mass Damping Systems”. *IEEE Transactions on Control Systems Technology*, 21 (4): 1090-1104. https://doi.org/10.1109/TCST.2013.2260825

Wu, Jong-Cheng, Ming-Hsiang Shih, Yuh-Yi Lin, and Ying-Chang Shen. 2005. “Design Guidelines for Tuned Liquid Column Damper for Structures Responding to Wind”. *Engineering Structures*, 27 (13): 1893-1905. https://doi.org/10.1016/j.engstruct.2005.05.009

Xue, Mi-An, Peng Dou, Jinhai Zheng, Pengzhi Lin, and Xiaoli Yuan. 2022. “Pitch Motion Reduction of Semisubmersible Floating Offshore Wind Turbine Substructure Using a Tuned Liquid Multicolumn Damper”. *Marine Structures*, 84: 103237. https://doi.org/10.1016/j.marstruc.2022.103237

Yalla, Swaroop K., and Ahsan Kareem. 2000. “Optimum Absorber Parameters for Tuned Liquid Column Dampers”. *Journal of Structural Engineering*, 126: (8), 906-915. https://doi.org/10.1061/(ASCE)0733-9445(2000)126:8(906)

Yalla, Swaroop K., and Ahsan Kareem. 2003 "Semiactive tuned liquid column dampers: experimental study." *Journal of Structural Engineering* 129, no. 7: 960-971. https://doi.org/10.1061/(ASCE)0733-9445(2003)129:7(960)

Yalla, Swaroop K., Ahsan Kareem, and Jeffrey C. Kantor. 2001. “Semi-active Tuned Liquid Column Dampers for Vibration Control of Structures.” *Engineering Structures*, 23 (11): 1469-1479. https://doi.org/10.1016/S0141-0296(01)00047-5

Yu, Wei, Frank Lemmer, and Po Wen Cheng. 2023. “Modeling and Validation of a Tuned Liquid Multi-column Damper Stabilized Floating Offshore Wind Turbine Coupled System”. *Ocean Engineering*, 280: 114442. https://doi.org/10.1016/j.oceaneng.2023.114442

Zuo, Haoran, Kaiming Bi, and Hong Hao. 2017. “Using Multiple Tuned Mass Dampers to Control Offshore Wind Turbine Vibrations Under Multiple Hazards.” *Engineering Structures*, 141: 303-315. https://doi.org/10.1016/j.engstruct.2017.03.006

APPENDICES

APPENDIX A- Visual of Experimental Desing

A camera is located across the experimental setup to record oscillations of the structure during experiments, as shown in Figure A.1. These records are exported to Tracker video analysis and modeling tools to determine the damping effect of the orifices.

Figure A.1 Visual of experimental design.

APPENDIX B- Video Analysis Process

Tracker video analysis and modeling tools were used to determine the displacement time story of the top of the structure. A red object located at the top of the structure is followed up while the structure oscillates, and the displacement time story of this red object can be plotted through Tracker as shown in Figure B.1.

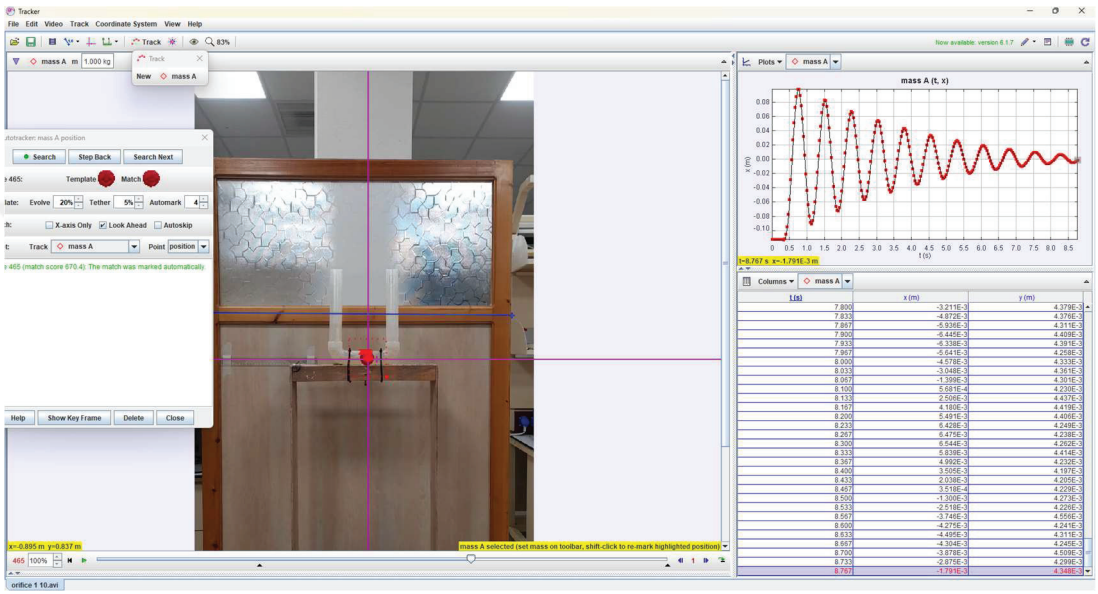

Figure B.1 Visual from tracker screen.

APPENDIX C- Python Code for Solution of Analytical Modeling

The analytical model was produced with respect to the equation of motions for TLCD and structure. An appropriate numerical method was applied to the coupled systems equation of motion. All calculations were completed using the below Python Code which was generated concerning the calculation procedure and solution algorithm.

Differential equations were solved using this code step by step and displacement, velocity, and acceleration plots were obtained for both TLCD and structure with respect to time. These values were also exported as Excel files.

```
import numpy as np
import matplotlib.pyplot as plt
import pandas as pd
import xlsxwriter
#----Geometry of U-shape tube-----
b=..... #----horizontal distance between two edge of U tube
l=..... #----total liquid length of U tube
r=..... #----radius of cross-sectional section
Area=np.pi*r**2 #----cross sectional area of tube
w=(2*9.81/l)**0.5 #----frequency of TLD
t0=0 #----time that includes force applied
t1=..... #----time without force
x0=0
v0=0
a0=0
X0=0
V0=0
A0=0
M=.....
C=.....
K=.....
Ccr = 2* np.sqrt(M*K)
W = np.sqrt(K/M)
Head loss value (ksi) = .....
d=1000 #----density of liquid
h=0.00.... #----increment value (Period/20)
f=0
time=0
n=int((t1)/h)
m= 1 * d*Area*l
mh=m*b/l #----mass of liquid
c=0
k=2*d*Area*9.81 #----stiffness of TLCD

ccr=2*m*w #----Critical damping value of TLCD
```

```
B=0 #----Ratio of the natural frequency and excitation frequency
DMF=0
X_values = [] # List to store X values
time_values = [] # List to store time values
for i in range (n):
P= 0 * np.cos(5*W*time)
X=((P-mh*a0)+(6*(M+m)/h**2)*(X0+V0*h+A0*(h**2/3))+
C*(3/h*X0+2*V0+A0*h/2))/((6*(M+m)/h**2)+(3*C/h)+K)
V=(X-X0)*(3/h)-2*V0-A0*h/2
A=(X-X0-V0*h-A0*(h**2/3))*(6/h**2)
f = 1 * -mh * A0
X_values.append(X) #Append current X value to the list
time_values.append(time) #Append current time value to the list
c=(ksi)*0.5*d*Area*np.absolute(v0)
x=f+(6*m/h**2)*(x0+v0*h+a0*(h**2/3))+c*(3/h*x0+2*v0+a0*h/2))/((6*m/h**2)+(3*
c/h)+k)
v= 1 * (x-x0)*(3/h)-2*v0-a0*h/2
a= 1 * (x-x0-v0*h-a0*(h**2/3))*(6/h**2)
damping=c*v
Damping_ratio=C/Ccr
damping_ratio=c/ccr
DMF= ((1-B**2)**2+(2*Damping_ratio*B)**2)**-1
B=B+2/n
print( X )
time=time+h
x0=x
v0=v
a0=a
X0=X
V0=V
A0=A
xpoints=time
ypoints=x
plt.subplot(1,3,1)
plt.title('TLCD response')
plt.xlabel('time')
plt.plot(xpoints, ypoints,'b.')
ypoints=X
plt.subplot(1,3,2)
plt.title('structure response')
plt.xlabel('time')
plt.plot(xpoints, ypoints,'r.')
xpoints=B
ypoints=DMF
plt.subplot(1,3,3)
plt.title('DMF')
plt.xlabel('Beta')
plt.plot(xpoints, ypoints,'g.')
# Convert X_values list and time_values list to a pandas DataFrame
df_X = pd.DataFrame({'Time': time_values, 'Displacement_X': X_values})
```

```
# Save DataFrame to a CSV file
df_X.to_csv('X_data.csv', index=False)
print(ksi,k,m,w,W)
plt.show()
```